Volume 11 | Number 16 | 21 August 2024

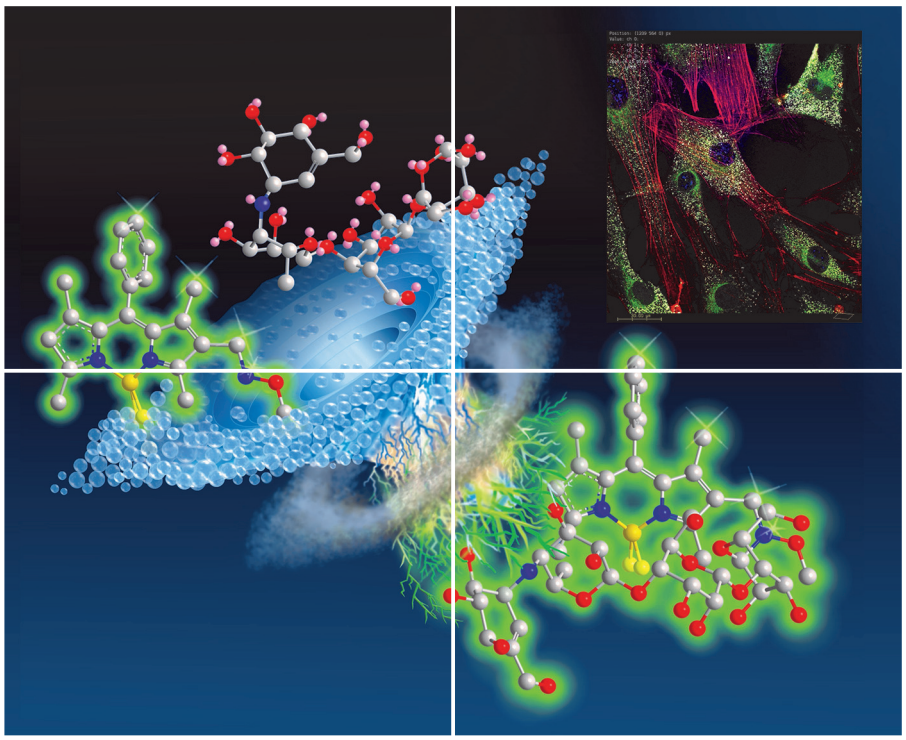

ORGANIC CHEMISTRY

FRONTIERS

CCS 中国化学会 CHINESE CHEMICAL SOCIETY

SIOC 1950

ROYAL SOCIETY OF CHEMISTRY

rsc.li/frontiers-organic

ORGANIC CHEMISTRY FRONTIERS

RESEARCH ARTICLE

View Article Online
View Journal | View Issue

Cite this: *Org. Chem. Front.*, 2024, **11**, 4356

Chemoselective reaction of methoxyaminomethyl BODIPYs with unprotected carbohydrates: a powerful tool for accessing BODIPY neoglycosides†

Ana M. Gómez, *[a] Luis García-Fernández, [b,c] Andrés G. Santana, [a] Clara Uriel,[a] Leire Gartzia-Rivero, [d] Jorge Bañuelos, *[d] Inmaculada Garcia-Moreno,[e] Lourdes Infantes, [f] María Rosa Aguilar [b,c] and J. Cristobal Lopez *[a]

Received 17th May 2024,
Accepted 22nd June 2024

DOI: 10.1039/d4qo00886c

rsc.li/frontiers-organic

The neoglycosylation of methoxyaminomethyl-appended BODIPYs with unprotected reducing mono-, di-, and trisaccharides produces, in a regio- and stereoselective manner, cyclic *N*-glycosyl-*N*-methoxy–BODIPY conjugates, as a relevant class of neoglycosides that display excellent photophysical characteristics in pure water, even at high dye concentrations. In addition, the cellular uptake of some of the neoglycosylated BODIPYs has been confirmed *via* fluorescence microscopy, and a BODIPY–acarbose conjugate showed comparable enzymatic inhibitory activity to acarbose for two different α-amylases: *A. oryzae* α-amylase (AOA) and human salivary α-amylase (HSA).

Introduction

Carbohydrates, ubiquitous in Nature, play significant roles in many biological processes ranging from infection (viral and bacterial), cell recognition, triggering of immune responses, and cancer metastasis.[1] In recent years, it has also become clear that carbohydrate–protein interactions involving cell surface proteins,[2] or cell surface carbohydrates,[3] are key to health and disease mechanisms.[4,5] The investigation of these processes, which falls under the umbrella of Glycobiology[6] is, therefore, a field attracting increasing interest. In this context, fluorescence imaging techniques have become powerful tools for the visualization of biomolecules, and the assessment of these phenomena. Such studies often require the derivatization of glycans by labeling with fluorophores[7] or by attachment to surfaces.[8] In this context, difluoroboron dipyrromethene (4,4-difluoro-4-bora-3a,4a-diaza-*s*-indacene) or BODIPY dyes, *e.g.*, **1** (Fig. 1A),[9] have arguably become one of the most popular fluorophores for saccharide tagging.[7b,10] BODIPYs display relatively high photostability, neutral total charge, sharp absorption and emission spectra, notable chemical robustness, and high fluorescence quantum yield (Φ_F).[9] More interestingly, all of the above properties can be modulated by subtle postfunctional modifications of the dipyrromethene core.[11,12] Thus, incorporating diverse functional groups to the BODIPY core can fine-tune the absorption and emission wavelengths of these dyes. This tunability enables the design of BODIPY derivatives with tailored fluorescence properties, making them suitable for various applications.[13] BODIPY derivatives possess many ideal photosensitizer (PS) features, which makes them useful agents in photodynamic therapy (PDT),[14] and, more recently, in photothermal therapy (PTT).[15] They have also been used in optoelectronic devices, including organic light-emitting diodes (OLEDs)[16] and organic photovoltaics (OPVs).[17] Derivatives of BODIPY are frequently used in biological imaging.[18] Their fluorescence makes them excellent for observing cellular structures, biomolecule distribution within cells, and dynamics.[19]

In this regard, because of their wide range of uses, adjustable fluorescence characteristics, and photostability, luminescent BODIPY–sugar probes have gained the attention of

[a]*Instituto de Química Orgánica General (IQOG-CSIC), Juan de la Cierva 3, 28006 Madrid, Spain. E-mail: ana.gomez@csic.es, jc.lopez@csic.es*
[b]*Instituto de Ciencia y Tecnología de Polímeros (ICTP-CSIC), Juan de la Cierva 3, 28006 Madrid, Spain*
[c]*Centro de Investigación Biomédica en Red de Bioingeniería, Biomateriales y Nanomedicina (CIBER-BBN), Instituto de Salud Carlos III, Monforte de Lemos 3-5, 28029 Madrid, Spain*
[d]*Departamento de Química Física, Universidad del País Vasco (UPV/EHU), Apartado 644, 48080 Bilbao, Spain. E-mail: jorge.banuelos@ehu.eus*
[e]*Departamento de Química-Física de Materiales, Instituto de Química-Física "Blas Cabrera" (IQF-CSIC), Serrano 119, 28006 Madrid, Spain*
[f]*Departamento de Cristalografía y Biología Estructural, Instituto de Química-Física "Blas Cabrera" (IQF-CSIC), Serrano 119, 28006 Madrid, Spain*

†Electronic supplementary information (ESI) available. CCDC 2351271. For ESI and crystallographic data in CIF or other electronic format see DOI: https://doi.org/10.1039/d4qo00886c

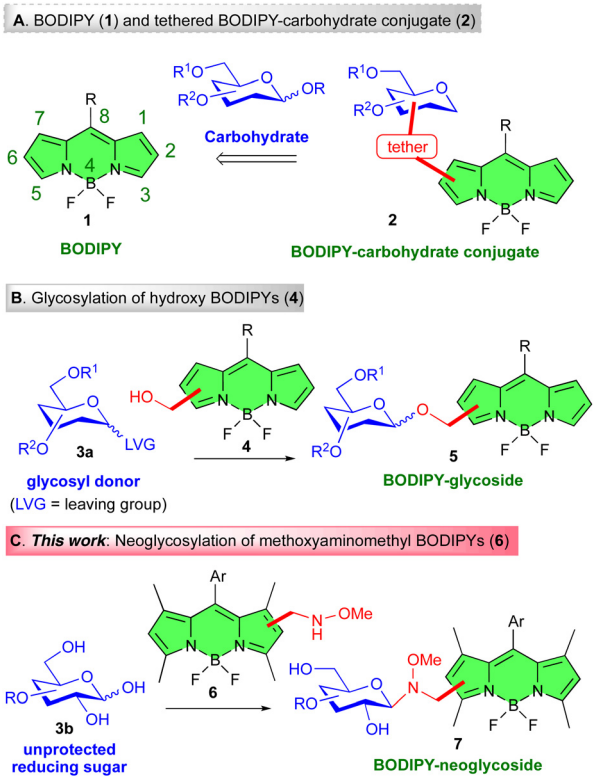

Fig. 1 (A) BODIPY (**1**) and tethered BODIPY–carbohydrate conjugates (**2**). (B) Glycosylation of hydroxyl-containing BODIPYs (**4**) with glycosyl donors **3a**, leading to BODIPY glycosides **5**. (C) Reaction of methoxyaminomethyl BODIPYs **6**, with unprotected reducing sugars **3b**, leading to BODIPY-neoglycosides **7**.

researchers for the potential applications of such molecular systems in bio-imaging.[20] The carbohydrate component of BODIPY–carbohydrate conjugates plays an important role since it confers remarkable properties to the BODIPY glycoprobes. Thus, the sugar component provides enhanced solubility in polar solvents (including water),[21] biocompatibility,[22] targeting ability,[23] cell endocytosis,[24] and, in some instances, reduced toxicity[25] to the glyco-fluorophores.[7,8]

In a broad sense, BODIPY–carbohydrate conjugates can be divided into linker-free or tethered derivatives. Classically, synthetic routes to the former class have been less exploited,[10,21,26] and attention has been mainly devoted to the synthesis of BODIPY–carbohydrate conjugates connected through a "linker". Among the latter, synthetic approaches to tethered BODIPY–carbohydrate hybrids, *e.g.*, **2** (Fig. 1A), often rely on the use of click reactions, in particular the copper(I)-catalyzed azide–alkyne cycloaddition (CuAAC)[27] on azido- or alkynyl BODIPYs.[28,29] On the contrary, methods based on carbohydrate transformations, for instance, the glycosylation of hydroxyl-appended BODIPYs, *e.g.*, **4**, with glycosyl donors **3a**, leading to glycosyl BODIPYs **5** (Fig. 1B),[30] have been scarcely employed.[31]

Seeking a powerful method to covalently link BODIPYs and carbohydrates, we were mindful of the seminal contribution by Peri, Dumy and Mutter,[32] which reported the regio- chemo- and stereoselective formation of glycosidic bonds between unprotected reducing sugars, *e.g.* **3b** (Fig. 1C), and secondary methoxyamine-containing aglycons. This transformation provides access to cyclic *N*-glycosyl-*N*,*O*-dialkyl neoglycosides in the thermodynamically most stable configurations.[33] These derivatives display conformational behavior similar to natural *O*-glycosides.[34] This ligation method, further validated by Langenhan and Thorson,[35] has proven useful in the preparation of bioactive probes and early-stage leads in drug discovery.[36]

Along these lines, we report in this manuscript the preparation of methoxyaminomethyl BODIPY dyes, *i.e.*, **6**, and their reaction with unprotected reducing sugar derivatives *e.g.*, **3b**, to afford BODIPY-neoglycosides, *i.e.*, **7** (Fig. 1C). Specifically, the method is applied to different methoxyaminomethyl BODIPY compounds as well as to saccharides of different chain lengths. The ensuing BODIPY conjugates displayed excellent photophysical properties in water and at high dye concentrations. Furthermore, some of these conjugates were submitted to biological studies including cellular uptake, intracellular localization, and cytotoxicity in healthy and tumoral cells. One of the sugar derivatives employed in these studies has been acarbose. Acarbose, an α-amylase and α-glucosidase inhibitor, exerts a well-defined glucoregulatory effect. Cancer cells are known to exhibit a heightened dependence on glucose for ATP production compared to their non-malignant counterparts.[37] Consequently, targeting this metabolic pathway by restricting glucose availability represents a well-established strategy in cancer therapy.[38–40] Finally, the acarbose–BODIPY conjugate was also evaluated as a chromogenic inhibitor of α-amylases.

Results and discussion

To evaluate the feasibility, scope and limitations of this approach, we initiated our studies with the preparation of methoxyaminomethyl BODIPYs **6a–c** (Fig. 2). These fluorescent dyes are derived from 8-aryl, 1,3,5,7 tetramethyl BODIPYs. In these compounds the methyl groups at C-1 and C-7 force the 8-aryl group to adopt an orthogonal orientation relative to the BODIPY core.[31a] This arrangement prevents unwanted aggregation and restricts the rotation of the aryl substituent, thereby preserving the chromophore's emission properties. In addition, the presence of the aryl and methyl groups in the BODIPY framework has a beneficial effect on its photostability and chemical robustness.[31b]

Our synthetic strategy began by reacting previously described formyl BODIPYs **8a**,[41] **8b**,[42] and **8c**,[31a] with methoxyamine hydrochloride salt using pyridine as a mediator (Fig. 2). This produced the corresponding BODIPY-*O*-methyl oximes **9a–c** in good yields (81%, 84%, and 74%, respectively).[43] Compounds **9a** and **9b** were obtained as single stereoisomers while **9c** exhibited a 6 : 1 mixture of isomers at the oxime double bond, as determined by ^{1}H-NMR spectroscopy.

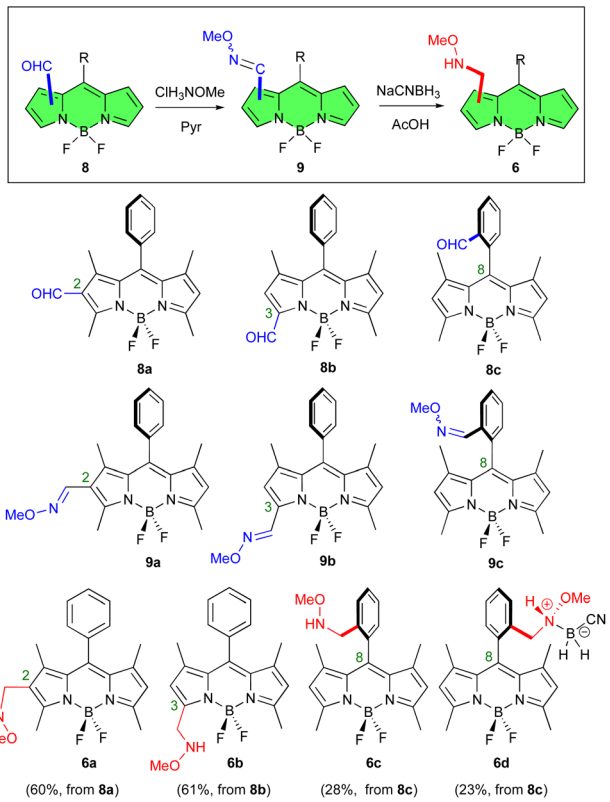

Fig. 2 Methoxyaminomethyl BODIPY derivatives **6a–d**, obtained from formyl-BODIPYs **8a–c**, *via* BODIPY oximes **9a–c**.

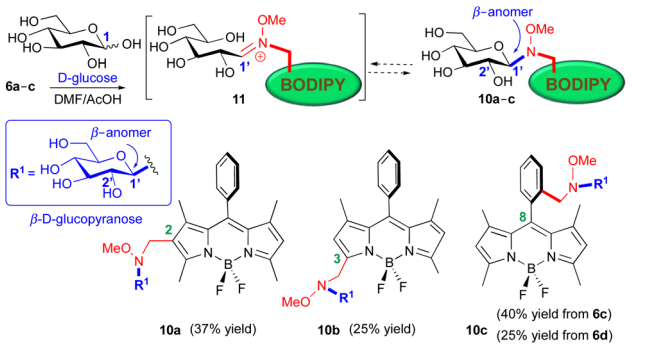

Fig. 3 Stereoselective synthesis of BODIPY neoglucosides **10a–c**, from the reaction of methoxyaminomethyl BODIPYs **6a–d** with D-glucose (DMF/AcOH, r.t.).

Reduction of the *O*-methyl oximes **9a–c** with $NaCNBH_3$ in glacial acetic acid then gave the expected methoxyaminomethyl BODIPYs **6a**, **6b** and **6c** in fair to good yields (74%, 73% and 38%, respectively, Fig. 2). In the latter case, the zwitterionic *N*-cyanoboronated-*N*-alkoxyamine derivative **6d** was also isolated (32% yield) as a crystalline derivative (Fig. 2).[44] This boronated species was characterized by NMR spectroscopy, mass spectrometry, and single crystal X-ray crystallography. The ^{1}H-NMR spectrum of compound **6d** showed benzylic protons that appeared as diastereotopic signals, due to the chiral nitrogen atom at the benzylic position. X-Ray diffraction confirmed that compound **6d** crystallized as a racemic compound (Fig. S84 in ESI†).

Next, we tested the compared reactivity of methoxyaminomethyl BODIPY derivatives **6a–d** in the neoglycosylation reaction using D-glucose as the glycosyl donor.[45] Thus, treatment of methoxyaminomethyl BODIPYs **6a–c**, under the reaction conditions initially recommended by Peri *et al.* (DMF/AcOH, r.t.),[32] resulted in the synthesis of glucosyl derivatives **10a**, **10b**, and **10c** in 37%, 25% and 40% yields, respectively (Fig. 3). Similarly, neoglycosylation of *N*-cyanoboronated-*N*-methoxyamine **6d**, with D-glucose yielded derivative **10c** in a slightly lower yield (25%, Fig. 3).

In agreement with literature precedents,[32] the glycosylation of *N*,*O*-disubstituted secondary hydroxylamino BODIPYs (**6**) with D-glucose took place in a completely regio- and stereocontrolled manner, leading to the corresponding β-D-glucopyranosyl derivatives (**10a–c**), with the expected 1,2-*trans* stereoselectivity on the carbohydrate moiety (Fig. 3).

The β-configuration at the BODIPY-attached anomeric carbon was rigorously established for compounds **10a–c**, on the basis of their observed $J_{1',2'}$ coupling constants in their ^{1}H-NMR spectra. In the case of compound **10b**, with no overlapping with other proton signals, the observed diagnostic coupling constant (4.16 ppm, $J_{1',2'}$ = 9.0 Hz) could be determined from its ^{1}H-NMR spectrum. On the contrary, the stereochemical assignment of the C-1′ configuration in *gluco*-BODIPYs **10a** and **10c** had to be carried out in their corresponding per-*O*-acetyl derivatives, **10a-OAc** and **10c-OAc** (see ESI† for details), where the improved splitting of the proton signals allowed the unequivocal assignment of their anomeric protons.

The stereoselection of the process has been ascribed to a thermodynamic equilibrium between the open iminium intermediate, *i.e.*, **11**, and the closed ring isomer, *i.e.*, **10**, in its most stable form (Fig. 3).[32,36]

Having established that all three methoxyamino BODIPYs (**6a–c**) could be used as aglycons in the neoglycosylation reaction, we then set up to optimize the reaction conditions for glycosyl coupling using BODIPY **6a** and D-glucose as partners. Compound **6a** was selected owing to the easiness of its preparation and its observed improved reactivity toward D-glucose, under the assumption that the results obtained with this compound could be extended to isomeric BODIPYs **6b** and **6c**.

Accordingly, we examined a variety of reaction conditions for the transformation **6a** → **10a** (Table 1).[36] In general, the different methods evaluated involved changes in the solvent system, temperature (T), and catalyst. Thus, the use of DMF/AcOH (1 : 1) solvent mixtures led to modest yields of **10a**, which could be slightly improved by increasing the reaction temperature (compare entries *i* and *ii*, r.t. *vs.* 40 °C, Table 1). The use of MeOH/CH_2Cl_2 (6 : 1) as a solvent system, in the absence of acid, produced a modest 25% yield of **10a** (Table 1, entry *iii*). The use of a AcONa/AcOH buffer, as the reaction media, did not result in the formation of **10a** (Table 1, entry

Table 1 Optimization of reaction conditions[a] for the preparation of neoglucoside **10a** by reaction of **6a** with D-glucose

Entry	Solvent(s)	T (°C)/t	Catalyst	Yield[b] (%)
i	DMF/AcOH (1 : 1)	r.t./20 h	—	37
ii	DMF/AcOH (1 : 1)	40 °C/20 h	—	40
iii	MeOH/CH_2Cl_2 (6 : 1)	60 °C/48 h	—	25
iv	AcONa/AcOH pH = 5	r.t./24 h	—	—
v	MeOH/AcOH (1 : 1)	60 °C/48 h	—	40
vi	MeOH/AcOH (1 : 1)	60 °C/1 h (MW)	—	73
vii	MeOH/AcOH (1 : 1)	60 °C/1 h (MW)	5-Methoxy-anthranilic acid	87

[a] Reaction conditions: **6a** (1.0 mmol), D-glucose (3.0 mmol). [b] Isolated yields.

iv). Better results were obtained when the neoglycosylation reaction was carried out in MeOH/AcOH (1 : 1) solvent mixtures. Thus heating (60 °C) of the reaction for 48 h produced a 40% yield of **10a** (Table 1, entry *v*). Interestingly, the use microwave irradiation (MW) allowed the reaction time to be reduced to 1 h, and the yield increased to 73% (Table 1, entry *vi*). Finally, best yields were obtained under microwave irradiation (MW, 60 °C, 1 h, 87% yield) in the presence of 5-methoxyanthranilic acid as nucleophilic catalyst, as suggested by Langenhan and coworkers (Table 1, entry *vii*).[46]

Likewise, the application of the optimized reaction conditions (MeOH/AcOH, 5-methoxyanthranilic acid cat., MW, 60 °C, 1 h) to methoxyamino BODIPYs **6b** and **6c**, allowed the preparation of glucoconjugates **10b** and **10c** in 76% and 84% yields, respectively (compare with yields displayed in Fig. 3).

To evaluate the scope of the method regarding the sugar donor, we studied the reaction of BODIPY **6a** with a variety of commercially available unprotected reducing sugars, including: (i) cellobiose, lactose, and maltose disaccharides, which differ in the configuration of their interglycosidic bond (β-*versus* α-, *e.g.*, cellobiose and lactose *versus* maltose); (ii) maltotriose as an example of a trisaccharide, and (iii) acarbose as a pseudotetrasaccharide. In each neoglycosylation reaction, the expected BODIPY-saccharides **12**, **13**, **14**, **15**, and **16**, respectively, with β-anomeric configuration at the linking position, could be isolated (Fig. 4). The β-configuration at the BODIPY-attached anomeric carbon in compounds **15** and **16** was rigorously established from their corresponding per-*O*-acetyl derivatives, **15-OAc** and **16-OAc** (see ESI† for details) on the basis of their observed $J_{1',2'}$ coupling constants in their ^{1}H-NMR spectra. On the other hand, the β-configuration at the BODIPY-attached anomeric carbon in compounds **12–14** was postulated in accordance with the literature precedents and the similarity with the related BODIPY glycosides prepared in this study, since only one isomer was isolated in each case.

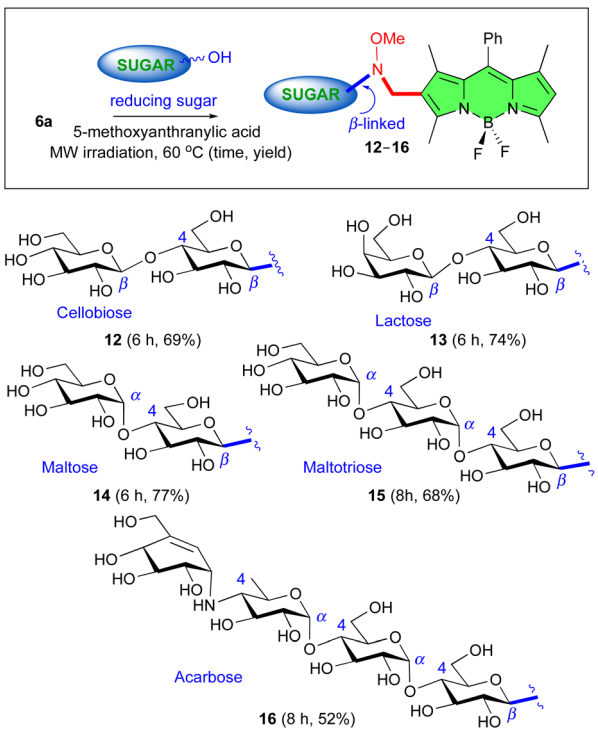

Fig. 4 Screening of carbohydrate substrates: stereoselective synthesis of BODIPY saccharides **12–16** by reaction of unprotected reducing sugars with BODIPY **6a**.

Photophysical studies

The photophysical features of the novel BODIPY glycoconjugates were next studied. The attachment of progressively complex carbohydrate units at C-2 of the BODIPY core, facilitated by the methoxyaminomethyl spacer, enhanced the hydrophilicity of the dye significantly, ultimately rendering it ready soluble in water. Indeed, the intrinsic photophysical properties of representative BODIPY glycoconjugates **10a** and **14–16** in diluted water solutions (Table 2) closely resembled those of their hydrophobic 8-phenyl BODIPY precursors (which lead to formyl dyes **8**).[32] Regardless of the number of carbohydrate

Table 2 Photophysical properties of representative BODIPY neoglycosides in water (dye concentration 2 μM)

Dye	λ_{ab}[a] (nm)	ε_{max}[b] × 10^4 (M^{-1} cm^{-1})	λ_{fl}[c] (nm)	ϕ[d]	τ[e] (ns)
10a	502.5	2.7	513.5	0.52	3.80
14	502.5	2.8	513.5	0.53	3.60
15	502.5	4.2	513.5	0.49	3.70
16	502.5	5.0	513.5	0.50	3.70

[a] Maximum absorption wavelength. [b] Maximum molar absorption. [c] Maximum fluorescence wavelength. [d] Fluorescence quantum yield. [e] Fluorescence lifetime.

units appended (ranging from one to four), these water-soluble dyes exhibited strong absorption and fluorescence bands in pure water (peaked at 502 nm and 513 nm, respectively, with molar extinction coefficients up to 50 000 M^{-1} cm^{-1} and 53% respectively, Table 2). Note that even at this low dye concentration, the parent 8-phenyl BODIPY was entirely insoluble and was prone to aggregate in aqueous solutions, resulting in the complete quenching of its fluorescent signal.[47]

To ensure the efficiency of these dyes as fluorescent bioprobes in physiological media, it is crucial to maintain their solubility and fluorescence response at higher concentrations. Thus, to assess the solubility and fluorescence performance of the BODIPY glycoconjugates at elevated concentrations in water, we studied the impact of dye concentration on their photophysical properties.

The incorporation of D-glucose or D-maltose to the BODIPY core, as in **10a** or **14**, respectively, facilitated the attainment of homogeneous water solutions up to 0.1 mM (Fig. 5). This water solubility was significantly enhanced by increasing the number of appended carbohydrate units, enabling the attainment of aqueous solution up to 1.9 mM in **15** with three sugar units (D-maltotriose), and even 2.4 mM grafting four sugar units (acarbose) in **16** (Fig. 5 and Fig. S85 in ESI†). However, at the highest concentration, the absorption profile of **15** and **16** became broader with a notable increase in the absorbance at shorter wavelengths (Fig. 5 and Fig. S85 in ESI†). According to the exciton model,[48] this spectral trend is indicative of H-type aggregation. Such aggregation should be a consequence of a weak exciton coupling, since its spectroscopic contribution arises as a shoulder of the main absorption band, even at the highest optical density (dye concentration around 2 mM for BODIPY conjugates **15** and **16**) herein tested in pure water. H-Aggregates are usually not fluorescent, as evidenced by both, a drastic decrease of the fluorescence efficiency (Fig. S87 in ESI†) and the absence of new emission bands in the fluorescence spectrum (Fig. 5). It is noteworthy that the observed increase of the long-wavelength shoulder in the fluorescence profile at this concentration was likely attributed to the reabsorption/reemission phenomena, which were not fully corrected solely by reducing the optical pathway in such highly concentrated media.[49]

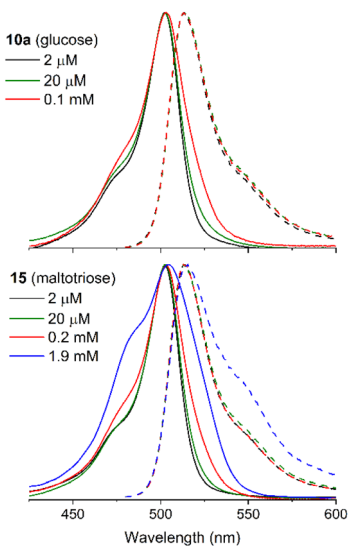

Fig. 5 Normalized absorption (solid line) and fluorescence (dashed line) spectra of BODIPY glycoconjugates **10a** and **15** bearing one and three carbohydrate units, respectively, as a function of the dye concentration in water using optically matched solutions (see ESI† for details). The spectra of BODIPY conjugates **14** and **16** are collected in Fig. S85 in ESI.† The recorded absorption spectra scaled by the molar absorption coefficient are collected in Fig. S86 in ESI.†

To quantify the impact of the aggregation and/or reabsorption/reemission phenomena on the fluorescence response, the absolute fluorescence quantum yields were estimated as a function of dye concentration (Fig. S87 in ESI†). As expected, an increase in dye concentration led to a decrease in fluorescence efficiency due to reabsorption and reemission effects (the optical path length was maintained at 1 mm for all dye concentrations) and the promotion of H-aggregates. Remarkably, all the BODIPY glycoconjugates retained a substantial fluorescence response (higher than 20%) at 0.1–0.2 mM concentrations, which are typical for the biological assays. Beyond this dye concentration, the fluorescence efficiency sharply decreased due to an increase in reabsorption/reemission and aggregation probabilities, which were enhanced at high optical densities, as shown in Fig. 5. Despite these adverse conditions, dyes **15** and **16** (bearing maltotriose and acarbose residues, respectively) still were able to retain a measurable fluorescence signal. Furthermore, their molar absorption coefficients were the highest ones recorded (almost double than those recorded for **10a** and **14**, bearing glucose and maltose respectively, Table 2). Consequently, an enhancement in the hydrophilicity of the BODIPY derivative is also evident in a more efficient harvesting of incoming excitation light, likely because the dye is better solvated and stabilized in the aqueous environment. These photophysical properties are expected to enhance the potential of BODIPYs **15** and **16** as bioprobes. In particular, the good solubility in pure water, without any hint of aggregation, and the bright fluorescence signal up to 0.1 mM, a concentration high enough for bioimaging essays in the aqueous cellular media, support this notion.

Toxicity on mammalian cells (healthy and tumor)

To analyze the toxicity of the different compounds on healthy and tumor cells, we conducted a toxicity test using healthy human breast epithelial cells (HMEpiC) and human breast adenocarcinoma epithelial cells (MCF-7, ECACC) (Fig. 6A and B, respectively). We observed that the toxicity of BODIPY-saccharides increased with the number of sugar units in both healthy and tumor cells. Regarding cytotoxic derivatives **15** and **16**, the former (maltotriose–BODIPY conjugate) displayed higher cytotoxicity against tumor cells (MCF-7) than against healthy human breast epithelial cells (HMEpiC) (Table 3). On the contrary, BODIPY–acarbose glycoconjugate (**16**), showed a different behavior, displaying similar LC_{50} against HMEpiC and MCF-7 cells (Fig. 7 and Table 3).

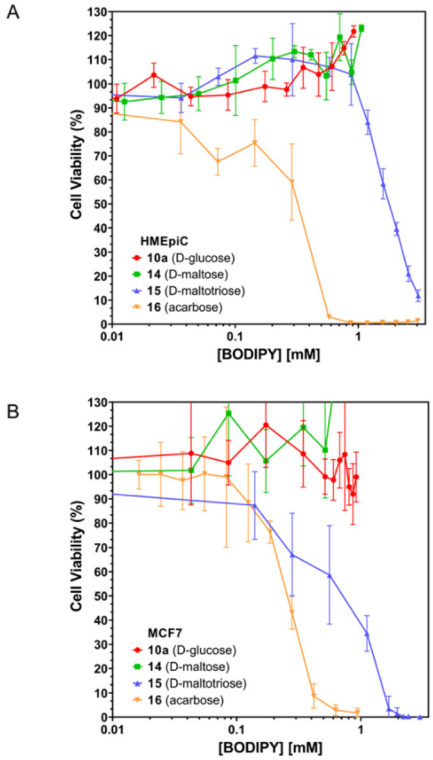

Fig. 6 Toxicity assays of BODIPY conjugates **10a** (D-glucose), **14** (D-maltose), **15** (D-maltotriose), and **16** (acarbose), on HMEpiC (A) and MCF-7 (B) cells.

Table 3 Observed LC_{50} value on healthy human breast epithelial cells (HMEpiC) and human breast adenocarcinoma epithelial cells (MCF-7, ECACC) of BODIPY–saccharide conjugates **15** and **16**

LC_{50} (mM)	**15** (D-maltotriose)	**16** (acarbose)
HMEpiC	1.8	0.32
MCF7	0.75	0.24

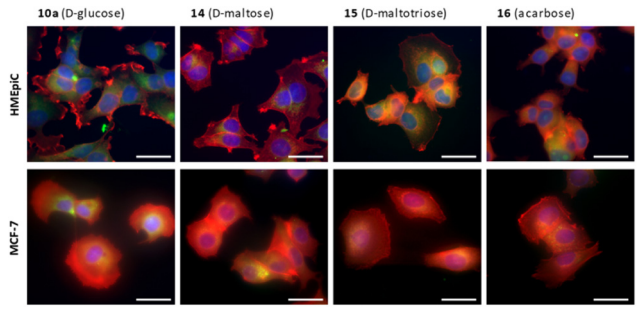

Fig. 7 Epifluorescence imaging of HMEpiC and MCF-7 cells showing BODIPYs internalization in green. Actin is marked in red and the nucleus in blue. Scale bar: 50 μm.

Cancer cells exhibit heightened glucose absorption and rely on an aerobic glycolytic pathway to fulfill their metabolic requirements for growth and proliferation. Targeting the inhibition of aerobic glycolysis presents a strategic therapeutic avenue to impede cancer cell progression.[40] In this sense, the use of acarbose or maltotriose could inhibit glucose uptake and promote glucose deprivation. In this way, both cell types showed the capacity to uptake the different BODIPYs derivatives (Fig. 7), which accumulated around the nucleus of the cell.

Cell internalization of BODIPY–acarbose conjugate 16

To evaluate cell internalization, BODIPY–acarbose conjugate **16** was selected due to its capacity to produce glucose deprivation.[40] We conducted several staining experiments. Lysosomes and mitochondria stains were performed together with actin and nucleus (Fig. 8, and Fig. S88–S90† for full-size pictures).

According to Fig. 8A, acarbose–BODIPY **16** is located near the nucleus but outside the mitochondria. The internalization process for **16** appears to be through the lysosomes as can be observed in Fig. 8B and C, and no accumulation was observed in the mitochondria. Lightning confocal microscopy (Fig. 8C) provides images to study spatiotemporal localization. The results showed a colocalization of the BODIPYs with the lysosomes and corroborate the capacity of cells to internalize acarbose–BODIPY **16**.

Enzymatic studies

To validate the neoglycosylation tagging protocol from an enzymatic perspective, we decided to study how the newly incorporated BODIPY appendage could affect the binding affinity of a

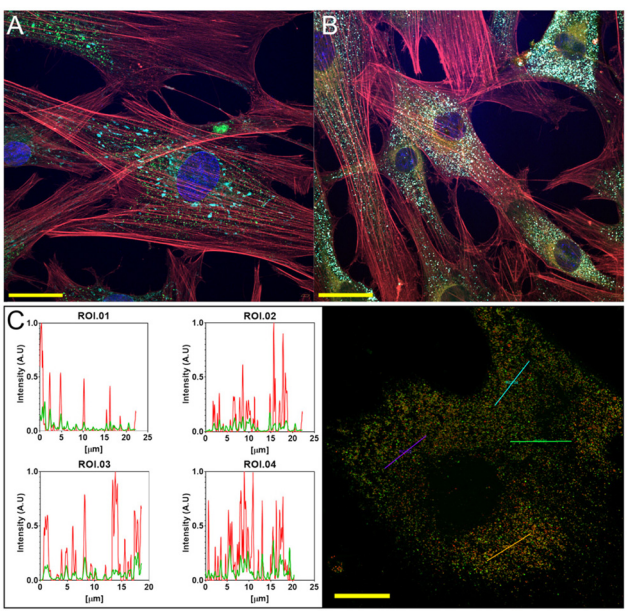

Fig. 8 (A) Confocal imaging of mitochondria (light blue), nucleus (blue), actin (red) stain and BODIPY internalization (green). Scale bar: 30 μm (B) confocal imaging of lysosomes (light blue), nucleus (blue), actin (red) stain and BODIPY internalization (green). Scale bar: 30 μm (C) lightning image and colocalization analysis of the lysosomes (red) and BODIPY (green). Scale bar: 20 μm.

Table 4 Inhibition kinetics results

IC_{50} (mM)	Acarbose	BODIPY–acarbose (**16**)
AOA	0.351	0.361
HSA	0.023	0.011

well-known amylase inhibitor, such as acarbose.[50] The latter is a pseudo-tetrasaccharide composed of an acarvosine unit, responsible for the inhibitory activity, which has been derivatized with D-maltose at the reducing end. With this purpose in mind, we tackled enzymatic inhibition studies of two different α-amylases: *A. oryzae* α-amylase (AOA) and human salivary α-amylase (HSA). The obtained IC_{50} values (Table 4) are in accordance with reported data,[51] confirm a dose-dependent competitive inhibition mode and reveal that the incorporation of the methoxyamino-BODIPY aglycon to acarbose, not only does not interfere with the inhibitory activity for AOA, but improves by two-fold the binding affinity for HSA. Overall, these results indicate that the neoglycosylation of selective enzymatic ligands with BODIPY dyes could be a convenient way to turn them into chromogenic probes with biological applications without affecting their inhibitory potency.

Conclusions

The neoglycosylation protocol used for the conjugation of BODIPYs to unprotected carbohydrate derivatives is a versatile and highly selective coupling method, which occurs under mild reaction conditions. The method can be applied to a variety of carbohydrate derivatives, including those with complex structures. The attachment of a sufficient number of saccharide units to the BODIPY core led to completely water-soluble dyes, retaining a high fluorescence signal even at high concentrations and hence suitable for use as fluorescent probes in physiological media. The biological studies of the BODIPY-neoglycosides showed excellent biocompatibilities and no cytotoxicity up to 0.1 mM of the probes. The cell's ability to uptake various BODIPY derivatives within a non-toxic range could have applications in various biological fields including bio-imaging. Specifically, the fluorescent acarbose–BODIPY conjugate **16** demonstrated the capability to be taken up by cells and localized within lysosomes, as evidenced by lighting confocal microscopy. This derivative also showed a binding affinity for α-amylases that is comparable to or better than that of acarbose alone, according to enzymatic activity studies. Accordingly, the uptake capacity combined with the PS features of BODIPY conjugates show promise in future biological applications in photodynamic and photothermal therapies.

Author contributions

A. M. G.: conceptualization, project administration, funding acquisition, writing – original draft, writing – review & editing. L. G. F.: investigation and writing – original draft. A. G. S.: investigation. C. U.: investigation and writing – original draft. L. G.-R.: investigation. J. B.: funding acquisition, supervising and writing. I. G.-M.: funding acquisition, supervising and writing. L. I.: investigation and funding acquisition. M. R. A.: investigation and funding acquisition. J. C. L.: conceptualization, funding acquisition, writing – original draft, writing – review & editing. All authors have read and agreed to the published version of the manuscript.

Conflicts of interest

There are no conflicts to declare.

Acknowledgements

This research received financial support from the Spanish *Ministerio de Ciencia e Innovación* (MCIN)/Agencia Estatal de Investigación (AEI) Grants: PID2020-114755GB-C31 and -C33, and PID2021-122504NB-I00 funded by MCIN/AEI/10.13039/501100011033 and by ERDF A way of making Europe. LGR and JB acknowledge Gobierno Vasco for financial support (IT1639-22). MRA and LGF acknowledge financial support from MCIN (PID2020-114086RB-I00) and *Comunidad de Madrid* (P2022/BMD-7406). MRA and LGF are members of the *SusPlast* platform from Consejo Superior de Investigaciones Científicas (*CSIC*). This research work was performed in the framework of the Nanomedicine *CSIC* HUB (ref 202180E048). The authors thank Ms. Rosa Ana Ramírez (*ICTP-CSIC*) for assistance in the biological experiments. We are also indebted to Ms. Marina Rodríguez and Mr Diego Raúl Pozas (*IQOG-CSIC*) for skilful technical support.

References

1 (*a*) A. Varki, Biological roles of oligosaccharides: all of the theories are correct, *Glycobiology*, 1993, **3**, 97–130; (*b*) A. Varki, R. Cummings, J. Esko, H. Freeze, G. Hart and J. Marth, *Essentials of Glycobiology*, Cold Spring Harbor Laboratory Press, New York, 2nd edn, 2009; (*c*) A. Varki, Biological Roles of Glycans, *Glycobiology*, 2017, **27**, 3–49.
2 K. Villadsen, M. C. Martos-Maldonado, K. J. Jensen and M. B. Thygesen, Chemoselective Reactions for the Synthesis of Glycoconjugates from Unprotected Carbohydrates, *ChemBioChem*, 2017, **18**, 574–612.
3 J. Ramos-Soriano, M. Ghirardello and M. C. Galan, Carbon-based glyco-nanoplatforms: towards the next generation of glycan-based multivalent probes, *Chem. Soc. Rev.*, 2022, **51**, 9960–9985.
4 J. E. Hudak and C. R. Bertozzi, Glycotherapy: New Advances Inspire a Reemergence of Glycans in Medicine, *Chem. Biol. Rev.*, 2014, **21**, 16–37.
5 S. Leusmann, P. Menova, E. Shanin, A. Titz and C. Rademacher, Glycomimetics for the inhibition and

modulation of lectins, *Chem. Soc. Rev.*, 2023, **52**, 3663–3740.

6 C. R. Bertozzi and L. L. Kiessling, Chemical Biology, *Science*, 2001, **291**, 2357–2364.

7 (*a*) X.-P. He, Y. Zang, T. D. James, J. Li, G.-R. Chen and J. Xie, Fluorescent glycoprobes: a sweet addition for improved sensing, *Chem. Commun.*, 2017, **53**, 82–90; (*b*) B. Thomas, K.-C. Yan, X.-L. Hu, M. Donnier-Marechal, G.-R. Chen, X.-P. He and S. Vidal, Fluorescent glycoconjugates and their applications, *Chem. Soc. Rev.*, 2020, **49**, 593–641; (*c*) X.-P. He and H. Tian, Lightening Up Membrane Receptors with Fluorescent Molecular Probes and Supramolecular Materials, *Chem*, 2018, **4**, 246–268; (*d*) M. Singh, M. Watkinson, E. M. Scanlan and G. J. Miller, Illuminating glycoscience: synthetic strategies for FRET-enabled carbohydrate active enzyme probes, *RSC Chem. Biol.*, 2020, **1**, 352–368.

8 Y. Chen, A. Star and S. Vidal, Sweet carbon nanostructures: carbohydrate conjugates with carbon nanotubes and graphene and their applications, *Chem. Soc. Rev.*, 2013, **42**, 4532–4542.

9 (*a*) A. Loudet and K. Burgess, BODIPY Dyes and Their Derivatives: Syntheses and Spectroscopic Properties, *Chem. Rev.*, 2007, **107**, 4891–4932; (*b*) R. Ziessel, G. Ulrich and A. Harriman, The chemistry of Bodipy: A new *El Dorado* for fluorescence tools, *New J. Chem.*, 2007, **31**, 496–501; (*c*) G. Ulrich, R. Ziessel and A. Harriman, The chemistry of fluorescent bodipy dyes: versatility unsurpassed, *Angew. Chem., Int. Ed.*, 2008, **47**, 1184–1201.

10 D. Kanyan, M. Horacek-Glading, M. J. Wildervanck, T. Söhnel, D. C. Ware and P. J. Brothers, *O*-BODIPYs as fluorescent labels for sugars: glucose, xylose and ribose, *Org. Chem. Front.*, 2022, **9**, 720–730.

11 (*a*) N. Boens, B. Verbelen, M. J. Ortiz, L. Jiao and W. Dehaen, Synthesis of BODIPY dyes through postfunctionalization of the boron dipyrromethene core, *Coord. Chem. Rev.*, 2019, **399**, 213024; (*b*) N. Boens, B. Verbelen and W. Dehaen, Postfunctionalization of the BODIPY Core: Synthesis and Spectroscopy, *Eur. J. Org. Chem.*, 2015, 6577–6595.

12 Y. Ni and J. Wu, Far-red and near infrared BODIPY dyes: synthesis and applications for fluorescent pH probes and bio-imaging, *Org. Biomol. Chem.*, 2014, **12**, 3774–3791.

13 Y. Fan, J. Zhang, Z. Hong, H. Qiu, Y. Li and S. Yin, Architectures and Applications of BODIPY-Based Conjugated Polymers, *Polymers*, 2021, **13**, 75.

14 (*a*) S. Das, S. Dey, S. Patra, A. Bera, T. Ghosh, B. Prasad, K. D. Sayala, K. Maji, A. Bedi and S. Debnath, BODIPY-Based Molecules for Biomedical Applications, *Biomolecules*, 2023, **13**, 1723; (*b*) J. Wang, Q. Gong, L. Jiao and E. Hao, Research advances in BODIPY-assembled supramolecular photosensitizers for photodynamic therapy, *Coord. Chem. Rev.*, 2023, **496**, 215367.

15 (*a*) J. Zou, P. Wang, Y. Wang, G. Liu, Y. Zhang, Q. Zhang, J. Shao, W. Si, W. Huang and X. Dong, Penetration depth tunable BODIPY derivatives for pH triggered enhanced photothermal/photodynamic synergistic therapy, *Chem. Sci.*, 2019, **10**, 268–276; (*b*) L. Schneider, M. Kalt, S. Koch, S. Sithamparanathan, V. Villiger, J. Mattiat, F. Kradolfer, E. Slyshkina, S. Luber, M. Bonmarin, C. Maake and B. Spingler, BODIPY-Based Photothermal Agents with Excellent Phototoxic Indices for Cancer Treatment, *J. Am. Chem. Soc.*, 2023, **145**, 4534–4544; (*c*) Z. Kang, W. Bu, X. Guo, L. Wang, Q. Wu, J. Cao, H. Wang, G. Yu, J. Gao, E. Hao and L. Jiao, Synthesis and Properties of Bright Red-to-NIR BODIPY Dyes for Targeting Fluorescence Imaging and Near-Infrared Photothermal Conversion, *Inorg. Chem.*, 2024, **63**, 3402–3410; (*d*) S. Lee, S. Min, G. Kim and S. Lee, Recent advances in the design of organic photothermal agents for cancer treatment: A review, *Coord. Chem. Rev.*, 2024, **506**, 215719.

16 H. Nakamura, S. Sasabe, K. Abe, K. R. Kumada, T. Sugiyama, J. Hanayama and M. Kido, Highly efficient and stable green fluorescent OLEDs with high color purity using a BODIPY derivative, *Mol. Syst. Des. Eng.*, 2023, **8**, 866–873.

17 D. Ho, R. Ozdemir, H. Kim, T. Earmme, H. Usta and C. Kim, BODIPY-Based Semiconducting Materials for Organic Bulk Heterojunction Photovoltaics and Thin-Film Transistors, *ChemPlusChem*, 2019, **84**, 18–37.

18 S. Koleman and E. U. Akkaya, Reaction-based BODIPY probes for selective bio-imaging, *Coord. Chem. Rev.*, 2018, **354**, 121–134.

19 T. Kowada, H. Maeda and K. Kikuchi, BODIPY-based probes for the fluorescence imaging of biomolecules in living cells, *Chem. Soc. Rev.*, 2015, **44**, 4953–4972.

20 (*a*) A. Barattucci, S. Campagna, T. Papalia, M. Galletta, A. Santoro, F. Puntoriero and P. Bonaccorsi, BODIPY on Board of Sugars: A Short Enlightened Journey up to the Cells, *ChemPhotoChem*, 2020, **4**, 647–658; (*b*) A. Barattucci, C. M. A. Gangemi, A. Santoro, S. Campagna, F. Puntoriero and P. Bonaccorsi, Bodipy-carbohydrate systems: synthesis and bioapplications, *Org. Biomol. Chem.*, 2022, **20**, 2742–2763.

21 A. M. Gomez, C. Uriel, A. Oliden-Sanchez, J. Bañuelos, I. Garcia-Moreno and J. C. López, A Concise Route to Water-Soluble 2,6-Disubstituted BODIPY-Carbohydrate Fluorophores by Direct Ferrier-Type *C*-Glycosylation, *J. Org. Chem.*, 2021, **86**, 9181–9188.

22 B. Kang, T. Opatz, K. Landfester and F. R. Wurm, Carbohydrate nanocarriers in biomedical applications: functionalization and construction, *Chem. Soc. Rev.*, 2015, **44**, 8301–8325.

23 (*a*) L. Shi, C. Yan, Y. Ma, T. Wang, Z. Guo and W.-H. Zhu, In vivo ratiometric tracking of endogenous β-galactosidase activity using an activatable near-infrared fluorescent probe, *Chem. Commun.*, 2019, **55**, 12308–12311; (*b*) N. E. M. Kaufman, Q. Meng, K. E. Griffin, S. S. Singh, A. Dahal, Z. Zhou, F. R. Fronczek, J. M. Mathis, S. D. Jois and M. G. H. Vicente, Synthesis, Characterization, and Evaluation of Near-IR Boron Dipyrromethene

Bioconjugates for Labeling of Adenocarcinomas by Selectively Targeting the Epidermal Growth Factor Receptor, *J. Med. Chem.*, 2019, **62**, 3323–3335; (*c*) W. Feng, S. Zhang, Y. Wan, Z. Chen, Y. Qu, J. Li, T. D. James, Z. Pei and Y. Pei, Nanococktail Based on Supramolecular Glyco-Assembly for Eradicating Tumors *In Vivo*, *ACS Appl. Mater. Interfaces*, 2022, **14**, 20749–20761; (*d*) G. Duran-Sampedro, E. Y. Xue, M. Moreno-Simoni, C. Paramio, T. Torres, D. K. P. Ng and G. de la Torre, Glycosylated BODIPY-Incorporated Pt(II) Metallacycles for Targeted and Synergistic Chemo-Photodynamic Therapy, *J. Med. Chem.*, 2023, **66**, 3448–3459.

24 T. Papalia, G. Siracusano, I. Colao, A. Barattucci, M. C. Aversa, S. Serroni, G. Zappala, S. Campagna, M. T. Sciortino, F. Puntoriero and P. Bonaccorsi, Cell internalization of BODIPY-based fluorescent dyes bearing carbohydrate residues, *Dyes Pigm.*, 2014, **110**, 67–71.

25 (*a*) L. Dong, Y. Zang, D. Zhou, X.-P. He, G.-R. Chen, T. D. James and J. Li, Glycosylation enhances the aqueous sensitivity and lowers the cytotoxicity of a naphthalimide zinc ion fluorescence probe, *Chem. Commun.*, 2015, **51**, 11852–11855; (*b*) F. Liu, P. Tang, R. Ding, L. Liao, L. Wang, M. Wang and J. Wang, A glycosylation strategy to develop a low toxic naphthalimide fluorescent probe for the detection of Fe3+ in aqueous medium, *Dalton Trans.*, 2017, **46**, 7515–7522.

26 (*a*) B. Liu, N. Novikova, M. C. Simpson, M. S. M. Timmer, B. L. Stocker, T. Söhnel, D. C. Ware and P. J. Brothers, Lighting up sugars: fluorescent BODIPY–glucofuranose and –septanose conjugates linked by direct B–O–C bonds, *Org. Biomol. Chem.*, 2016, **14**, 5205–5209; (*b*) L. J. Patalag, S. Ahadi, O. Lashchuk, P. G. Jones, S. Ebbinghaus and D. B. Werz, GlycoBODIPYs: Sugars Serving as a Natural Stock for Water-soluble Fluorescent Probes of Complex Chiral Morphology, *Angew. Chem., Int. Ed.*, 2021, **60**, 8766–8771; (*c*) C. Sollert, D. Kocsi, R. T. Jane, A. Orthaber and K. E. Borbas, *C*-glycosylated pyrroles and their application in dipyrromethane and porphyrin synthesis, *J. Porphyrins Phthalocyanines*, 2021, **25**, 741–755; (*d*) C. Uriel, D. Grenier, F. Herranz, N. Casado, J. Bañuelos, E. Rebollar, I. Garcia-Moreno, A. M. Gomez and J. C. Lopez, *De Novo* Access to BODIPY *C*-Glycosides as Linker-Free Nonsymmetrical BODIPY-Carbohydrate Conjugates, *J. Org. Chem.*, 2024, **89**, 4042–4065.

27 M. Meldal and C. W. Tornoe, Cu-catalyzed azide-alkyne cycloaddition, *Chem. Rev.*, 2008, **108**, 2952–3015.

28 M. R. Martinez-Gonzalez, A. Urias-Benavides, E. Alvarado-Martínez, J. C. Lopez, A. M. Gomez, M. del Rio, I. Garcia, A. Costela, J. Bañuelos, T. Arbeloa, I. Lopez Arbeloa and E. Peña-Cabrera, Convenient Access to Carbohydrate–BODIPY Hybrids by Two Complementary Methods Involving One-Pot Assembly of "Clickable" BODIPY Dyes, *Eur. J. Org. Chem.*, 2014, 5659–5663.

29 A. M. Gomez and J. C. Lopez, Bringing Color to Sugars: The Chemical Assembly of Carbohydrates to BODIPY Dyes, *Chem. Rec.*, 2021, **21**, 3112–3130.

30 X. Zhu and R. R. Schmidt, New Principles for Glycoside-Bond Formation, *Angew. Chem., Int. Ed.*, 2009, **48**, 1900–1934.

31 (*a*) M. del Rio, F. Lobo, J. C. Lopez, A. Oliden, J. Bañuelos, I. Lopez-Arbeloa, I. Garcia-Moreno and A. M. Gomez, One-Pot Synthesis of Rotationally Restricted, Conjugatable, BODIPY Derivatives from Phthalides, *J. Org. Chem.*, 2017, **82**, 1240–1247; (*b*) C. Uriel, C. Permingeat, J. Ventura, E. Avellanal-Zaballa, J. Bañuelos, I. Garcia-Moreno, A. M. Gomez and J. C. Lopez, BODIPYs as Chemically Stable Fluorescent Tags for Synthetic Glycosylation Strategies towards Fluorescently Labeled Saccharides, *Chem. – Eur. J.*, 2020, **26**, 5388–5399; (*c*) J. Ventura, C. Uriel, A. M. Gomez, E. Avellanal-Zaballa, J. Bañuelos, I. García-Moreno and J. C. Lopez, A Concise Synthesis of a BODIPY-Labeled Tetrasaccharide Related to the Antitumor PI-88, *Molecules*, 2021, **26**, 2909.

32 F. Peri, P. Dumy and M. Mutter, Chemo- and Stereoselective Glycosylation of Hydroxylamino Derivatives: A Versatile Approach to Glycoconjugates, *Tetrahedron*, 1998, **54**, 12269–12278.

33 F. Peri, A. Deutman, B. La Ferla and F. Nicotra, Solution and solid-phase chemoselective synthesis of (1–6)-amino (methoxy) di- and trisaccharide analogues, *Chem. Commun.*, 2002, 1504–1505.

34 F. Peri, J. Jimenez-Barbero, V. Garcia-Aparicio, I. Tvaroska and F. Nicotra, Synthesis and Conformational Analysis of Novel $N(OCH_3)$-linked Disaccharide Analogues, *Chem. – Eur. J.*, 2004, **10**, 1433–1444.

35 J. M. Langenhan, N. R. Peters, I. A. Guzei, F. M. Hoffmann and J. S. Thorson, Enhancing the anticancer properties of cardiac glycosides by neoglycorandomization, *Proc. Natl. Acad. Sci. U. S. A.*, 2005, **102**, 12305–12310.

36 R. D. Goff and J. S. Thorson, Neoglycosylation and neoglycorandomization: enabling tools for the discovery of novel glycosylated bioactive probes and early stage leads, *MedChemComm*, 2014, **5**, 1036–1047.

37 S. Romero-Garcia, J. S. Lopez-Gonzalez, J. L. Baez-Viveros, D. Aguilar-Cazares and H. Prado-Garcia, Tumor cell metabolism, *Cancer Biol. Ther.*, 2011, **12**, 939–948.

38 A. Gatenby and R. J. Gillies, Glycolysis in cancer: A potential target for therapy, *Int. J. Biochem. Cell Biol.*, 2007, **39**, 7–8.

39 R. M. Orlandella, W. J. Turbitt, J. T. Gibson, S. K. Boi, P. Li, D. L. Smith Jr. and L. A. Norian, The Antidiabetic Agent Acarbose Improves Anti-PD-1 and Rapamycin Efficacy in Preclinical Renal Cancer, *Cancers*, 2020, **12**, 2872.

40 Q. A. Obaid, A. M. Al-Shammari and K. K. Khudair, Glucose Deprivation Induced by Acarbose and Oncolytic Newcastle Disease Virus Promote Metabolic Oxidative Stress and Cell Death in a Breast Cancer Model, *Front. Mol. Biosci.*, 2022, **9**, 816510.

41 L. Jiao, C. Yu, J. Li, Z. Wang, M. Wu and E. Hao, β-Formyl-BODIPYs from the Vilsmeier-Haack Reaction, *J. Org. Chem.*, 2009, **74**, 7525–7528.

42 A. Ramos-Torres, E. Avellanal-Zaballa, A. Prieto-Castañeda, F. García-Garrido, J. Bañuelos, A. R. Agarrabeitia and M. J. Ortiz, FormylBODIPYs by PCC-Promoted Selective Oxidation of α-MethylBODIPYs. Synthetic Versatility and Applications, *Org. Lett.*, 2019, **21**, 4563–4566.

43 H. Ilhan and Y. Cakmak, Functionalization of BODIPY dyes with additional C-N Double Bonds and their applications, *Top. Curr. Chem.*, 2023, **381**, 28.

44 J. M. Márquez, E. Martínez-Castro, S. Gabrielli, O. López, I. Maya, M. Angulo, E. Álvarez and J. G. Fernández-Bolaños, Alkoxyamine-cyanoborane adducts: efficient cyanoborane transfer agents, *Chem. Commun.*, 2011, **47**, 5617–5619.

45 S. van der Vorm, T. Hansen, J. M. A. van Hengst, H. S. Overkleeft, G. A. van der Marel and J. D. C. Codee, Acceptor reactivity in glycosylation reactions, *Chem. Soc. Rev.*, 2019, **48**, 4688–4706.

46 S. A. Loskot, J. Zhang and J. M. Langenhan, Nucleophilic Catalysis of MeON-Neoglycoside Formation by Aniline Derivatives, *J. Org. Chem.*, 2013, **78**, 12189–12193.

47 A. B. Descalzo, P. Ashokkumar, Z. Shen and K. Rurack, On the aggregation behaviour and spectroscopic properties of alkylated and annelated Boron Dipyrromethene (BODIPY) dyes in aqueous solution, *ChemPhotoChem*, 2020, **4**, 120–131.

48 S. C. J. Meskers, The exciton model for molecular materials; past, present and future?, *ChemPhysChem*, 2023, **24**, e202300666.

49 H. B. Rodriguez, M. Mirenda, M. G. Lagorio and E. San Román, Photophysics at unusually high dye concentrations, *Acc. Chem. Res.*, 2019, **52**, 110–118.

50 (*a*) J.-L. Chiasson, R. G. Josse, R. Gomis, M. Hanefeld, A. Karasik and M. Laakso, Acarbose for prevention of type 2 diabetes mellitus: the STOP-NIDDM ransomised trial, *Lancet*, 2002, **359**, 2072–2077; (*b*) M. Qian, R. Haser, G. Buisson, E. Duée and F. Payan, The Active Center of a Mammalian α-Amylase. Structure of the Complex of a Pancreatic α-Amylase with a Carbohydrate Inhibitor Refined to 2.2-A Resolution, *Biochemistry*, 1994, **33**, 6284–6294.

51 M. Yilmazer-Musa, A. M. Griffith, A. J. Michels, E. Schneider and B. Frei, Grape Seed and Tea Extracts and Catechin 3-Gallates Are Potent Inhibitors of α-Amylase and α-Glucosidase Activity, *J. Agric. Food Chem.*, 2012, **60**, 8924–8929.